Geophys. J. R. astr. Soc. (1969) **19**, 113–146

Palaeomagnetic and Rock Magnetic Studies on the Cenozoic Basalts from Western Argentina

K. M. Creer and D. A. Valencio

(Received 1969 July 3)

Summary

Results are presented of a study of 234 samples of Cenozoic basalts from the extra-Andean region of the Provinces of Mendoza and Neuquén in the Argentine Republic, between latitudes 34° S and 40° S.

These basalts have been divided into seven groups of flows on the basis of their stratigraphy, ranging in age from the Miocene (Basalts I) to historic (Basalts VII).

The TRM of Basalts V, VI and VII is normally polarized and it is concluded that they belong to the Brunhes geomagnetic epoch. The TRM directions of Basalt IV flows are neither parallel nor antiparallel to the axial dipole field. These differences in direction are significant and persistent after cleaning. It is therefore suggested that Basalt IV was extruded during a magnetic transition after the Brunhes geomagnetic epoch. Some Basalt III flows are normally polarized, some are reversely polarized and some are magnetized obliquely to the axial dipole field. Hence the time of extrusion of these flows may span the Jaramillo and/or Olduvai events within the Matuyama epoch. Basalt II flows, which are stratigraphically placed in the Upper Pliocene, are all reversely magnetized while Basalt I flows, some of which are said to be Miocene, exhibit both normal and reversed polarities. It is deduced from the palaeomagnetism of these Basalts that some modifications should be made to their stratigraphy and these deductions have been substantiated by radiometric studies described in the following paper.

Estimates of the palaeosecular variation have been made for the Brunhes and Matuyama epochs and compared with other similar data from other parts of the world.

Ore microscope observations do not reveal any obvious correlation between polarity and state of oxidation, but a relationship between stability and the degree of exsolution is observed. Electron microprobe studies reveal a high titanium content: the unexsolved titanomagnetites have between 50 and 75 per cent ulvöspinel.

It is provisionally suggested that these characteristics of these basalts vary more in time than in geographical area at a given time.

1. Geology

These effusive rocks are exposed in the western part of Mendoza and Neuquén Provinces, Argentina, and samples were collected from the area contained between 69° W and 71° W meridians and 35° S and 40° S parallels. The numerous lava flows exposed in this area, principally basalts and andesites, have been classified in chronological order from I (Miocene) to VII (Holocene) by Groeber (1929, 1933, 1937,

Table 1

Stratigraphic succession of Argentine basalt flows

Basalt group	Local zone name	Geological period	Comments
VII	Ur. Tromelitense	Ur. Holocene	Last effusions ca. 500 yr ago
VI	Lr. Tromelitense	Ur. Holocene	
V	Puentelitense	Lr. Holocene	Post glacial
IV	Ur. Chapualitense	Ur. Pleistocene	
III	Lr. Chapualitense	M. Pleistocene	Before 2nd Andean glaciation
II	Coyocholitense	Ur. Pliocene	Followed 3rd Andean tectonic phase
I	Palaeocolitense	Miocene	Followed 2nd Andean tectonic phase

1946, 1947 and 1949). The relative positions of the different flows exposed in a given locality can be established simply by observation, but the attachment of ages (I to VII) has frequently only been established by analogy with Groeber's descriptions (see Table 1).

Basalt I (sometimes referred to as Palaeocolitense) is represented by a succession of flows of feldspathic basalt, frequently containing abundant olivine and sometimes associated with thick beds of breccias and tuffs. Groeber (1933) attributed the origin of these basaltic flows to eruptions following the second Andean tectonic phase during the Miocene. This age has been substantiated by the presence of Santa-Crucean fossils in tuffs contemporaneous with flows.

Basalt II (Coyocholitense) is supposed to be of Upper Pliocene age, corresponding to effusions which followed the third Andean tectonic phase. In the zone outside the cordillera, this basalt forms extensive tablelands which are cut by the erosion of streams because it was later strongly uplifted. It is often possible to recognize the skeletal remains of the volcanoes from which these flows were extruded.

Towards the end of the Pliocene, diastrophism produced a topography similar to the present one on which the products of a new effusive cycle accumulated in the Middle Pleistocene. Groeber (1933) named these flows Basalt III (Lower Chapualitense). They are highly eroded and generally exist singly, rarely forming successions of flows. The original volcanoes are well preserved. Groeber (1946) observed that many of the surfaces of these flows show evidence of having been polished by glaciers of the second Andean glaciation.

Later in the Quaternary (Upper Pleistocene) there was further uplift followed by a new series of eruptions named Basalt IV (Upper Chapualitense) by Groeber (1933, 1946). They are terraced and are often exposed at the bottoms of old valleys at lower topographic levels than Basalt III flows. Hence it is often difficult to distinguish flows of Basalt IV from those of Basalt II.

Basalts V (Puentelitense) are said to be post-glacial, probably Lower Holocene. They are fresh and cover a notably large area.

Basalt VI (Lower Tromelitense) and Basalt VII (Upper Tromelitense) are quite fresh and are said to be of Upper Holocene age. The most recent sequence of eruptions comprise Basalt VII, the last effusions of which, according to Indian folklore occurred at about the time of Columbus.

For the purpose of presentation and study, the sampling area has been divided into five parts, viz.

(a) '*Llancanelo*', the area situated to the north of latitude 36° S which contains flows outcropping south of River Malargue between Llancanelo lagoon and National Route No. 40 (R.N.40). It has been described by Criado Roque (1949) and Groeber (1947).

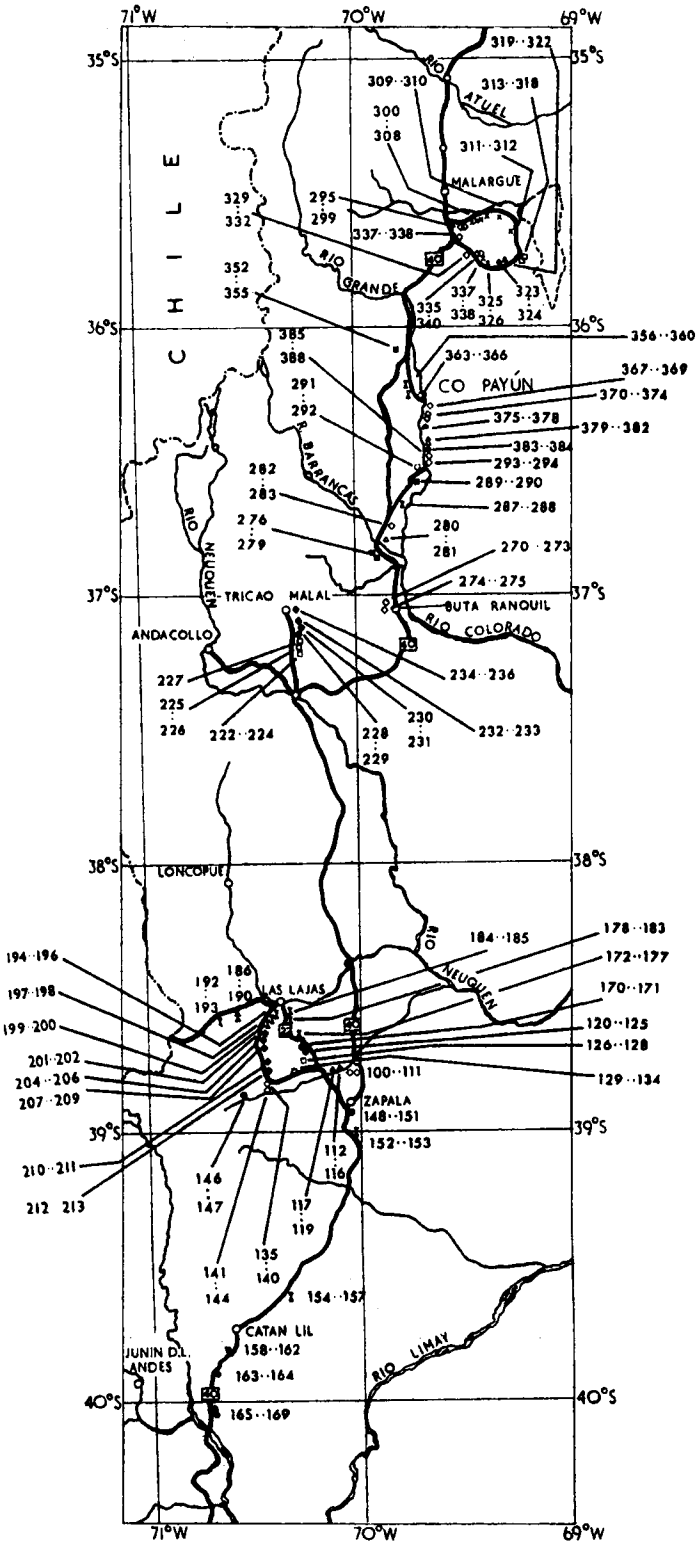

FIG. 1. Map showing sampling sites in the Provinces of Neuquén and Mendoza. The Basalt type is indicated by the shape of the symbol, viz. ◇ = Basalt VII, ⌓ = Basalt VI, ○ = Basalt V, □ = Basalt IV, △ = Basalt III, ⬡ = Basalt II, and × = Basalt I. Open symbols indicate 'normal' magnetization and solid symbols 'reversed' magnetization.

(b) '*Los Volcanes*', the area lying south of 36° S latitude and the parallel of latitude passing through the most southerly of the three bridges over the Rio Grande. It has been described by Groeber (1937 and 1947).

(c) '*Buta Ranquil*', the area lying between the latter parallel of latitude and 38° S and described by Groeber (1947) and by Zollner & Amos (1953).

(d) '*Zapala*', the area lying between latitudes 38° S and 39·5° S. This has been described by Groeber (1946) and a part by Lambert (1956).

(e) '*South Zapala*', the area lying to the south of latitude 39·5° S and stretching as far south as Zunin de los Andes.

This area has also been studied by geologists of Y.P.F. (the Argentine Oil Company) but their work is unpublished. Aerial photographs of the area are also in possession of Y.P.F.

The sampling sites are located in Fig. 1.

Previous palaeomagnetic studies on these lavas have been described, in English by Creer (1958) and in Spanish by Valencio (1965a and b) and Valencio and Creer (1968).

2. Sampling and measuring techniques

Cores were collected with a portable drill from some sites, from others, hand samples were collected. As a rule, orientation was measured with both sun compass and magnetic compass, but when the Sun was not shining only magnetic orientations were taken. Sampling sites within a given flow were selected at least 500 m from one another, three or four samples being collected at each site. The distance between samples was usually a few tens of metres.

One-inch cylinders were machined and their NRM M_0 measured with either an astatic or an air turbine driven spinner magnetometer, some in Newcastle and some in Buenos Aires. Most specimens were then subjected to A.F. demagnetization. From the curves of normalized remanence M/M_0 as a function of demagnetizing field H, two estimates of the coercivity of remanence were made, viz., H_{cb}, the value of demagnetizing field where the slope of the descending demagnetization curve starts to flatten off and H_{ca}, the field required to reduce the ratio M/M_0 to 0·5. In the majority of cases, the demagnetizing field H_{ca} was found to produce the best defined direction of remanence. Thermal demagnetization studies were also carried out, principally in an atmosphere of air, and blockage temperatures in the range (a) 130–200 °C and (b) 520–570 °C were found mainly.

3. Palaeomagnetic results

The results are summarized in Table 2 where the mean values of cleaned remanence (column 4) and polarity (column 5) for each area and age of basalt are listed. The directions of uncleaned NRM are plotted area by area in Figs 2–6 and the mean directions of hand samples after A.F. cleaning are illustrated in the stereograms which comprise Figs 7–11. In the following paragraphs the results obtained are commented on.

3.1. *Llancanelo area*

Basalts III, IV, V and VII were studied in this area. Basalts III, V and VII have normal polarity and are well grouped. Basalt IV in this area is magnetized in a transitional direction approaching reverse. See Figs 2 and 7.

3.2. *Los Volcanes area*

Basalts I, III, IV, V and VI were studied. All showed good grouping except Basalt IV whose mean direction is transitional, but closer to normal than reversed.

Table 2

Basalt group No.	Age given by geologists	Area of collection	Particulars of remanence after A.C. cleaning N	D	I	α	k	δ	Polarities	Polarity epoch deduced
VII	Ur. Holocene	Llancanelo	16	319°	−63°	13°	8·9	27·2	*N*	Brunhes
VI	Ur. Holocene	Los Volcanes	5	351°	−54°	6°	17·80	1·8	*N*	Brunhes
V	Lr. Holocene post-glacial	Llancanelo	14	356°	−60°	14°	8·9	27·2	*N*	Brunhes
		Los Volcanes	18	22°	−62°	14°	7·3	30·0	*N*	
		Buta Ranquil	13	12°	−62°	8°	34·4	13·8	*N*	
		Zapala	20	3°	−54°	9°	15·2	20·8	*N*	
		Tricao Malal	9	162°	+63°	15°	12·9	22·6	*R*	
IV	Ur. Pleistocene	Llancanelo	4	91°	+53°	27°	12·3	23·1	O(*R*)	Brunhes–Matuyama transition
		Los Volcanes	4	274°	−71°	77°	2·4	33·7	O(*N*)	
		Buta Ranquil	2	43°	−27°				O(*N*)	
		Zapala	23	176°	+56°	9°	13·6	22·0	*R*	
III	M. Pleistocene	Llancanelo	6	2°	−45°	12°	29·8	14·8	*N*	Matuyama–Jaramillo transitions or Matuyama–Olduvai transitions
		Los Volcanes	3	182°	+52°	10°	150·0	6·6	*R*	
		Buta Ranquil	6	149°	−78°	37°	7·2	30·2	O(*N*)	
		Buta Ranquil	6	187°	+71°	15°	36·1	13·5	*R*	
		Zapala	9	302°	−65°	21°	6·7	31·3	*N*	
		South Zapala	4	139°	+24°	17°	28·4	15·2	O(*R*)	
II	Ur. Pliocene	Zapala	13	163°	+57°	12°	12·1	23·2	*R*	Matuyama
		South Zapala	7	169°	+60°	10°	39·6	12·9	*R*	
I	Lr. Pliocene to Ur. Miocene	Los Volcanes	4	174°	+56°	13°	7·6	29·4	*R*	
		Zapala	9	338°	−71°	27°	4·5	38·2	*N*	
		Zapala	5	187°	+40°	31°	6·9	30·8	*R*	
		South Zapala	4	189°	+62°	12°	56·6	10·8	*R*	

N = Number of samples.
D = Declination; I = Inclination.
α = radius of 95 per cent circle of confidence.
k = precision.
δ = circular standard deviation.
Polarities: *N* = normal; *R* = reversed; O(*N*) = oblique, nearer normal O(*R*) = oblique, nearer reversed.

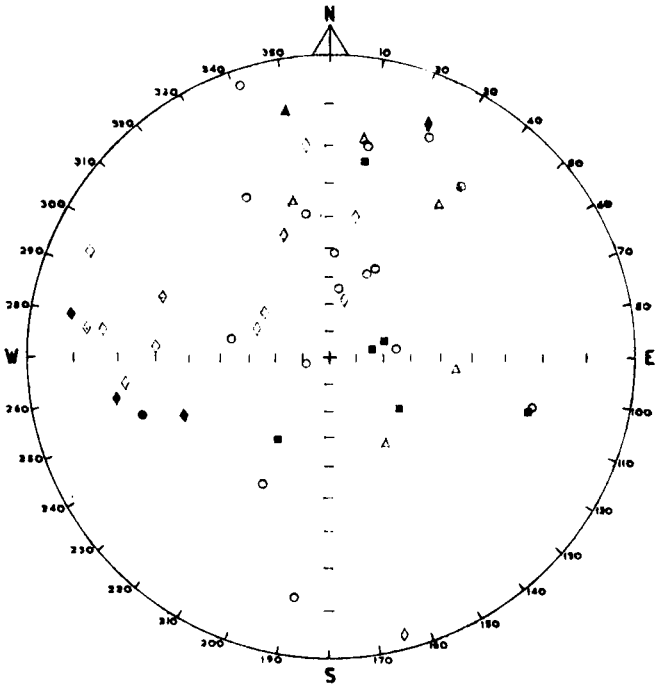

FIG. 2. *Llancanelo Area.* Uncleaned NRM directions of specimen cylinders of rock. Open symbols indicate upward dipping magnetization vectors (negative inclination) and solid symbols indicate downward dipping magnetizations (positive inclinations). The key to the symbols is as given in the caption to Fig. 1.

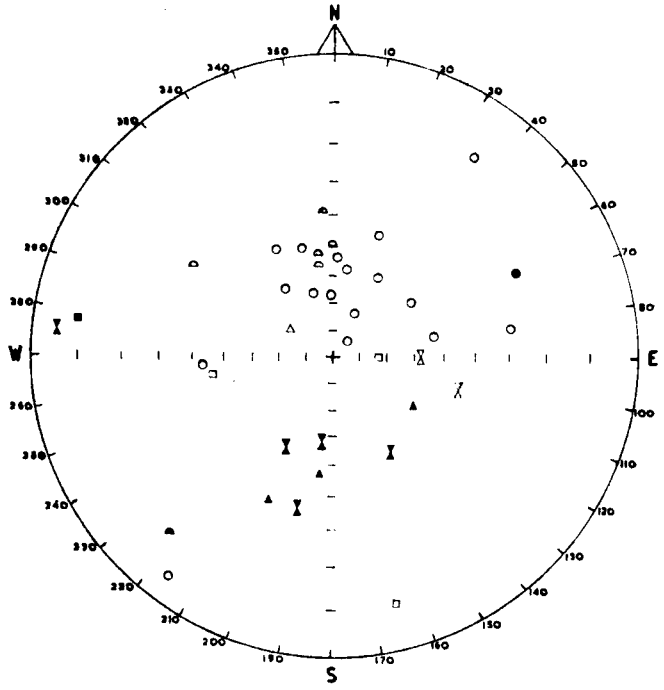

FIG. 3. *Los Volcanes Area.* Uncleaned NRM directions of specimen cylinders of rock.

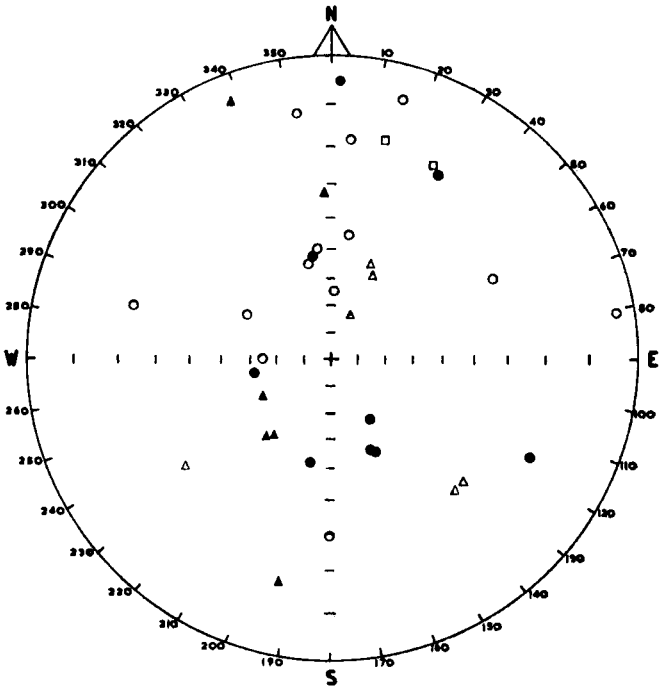

FIG. 4. *Buta Ranquil Area.* Uncleaned NRM directions of specimen cylinders of rock.

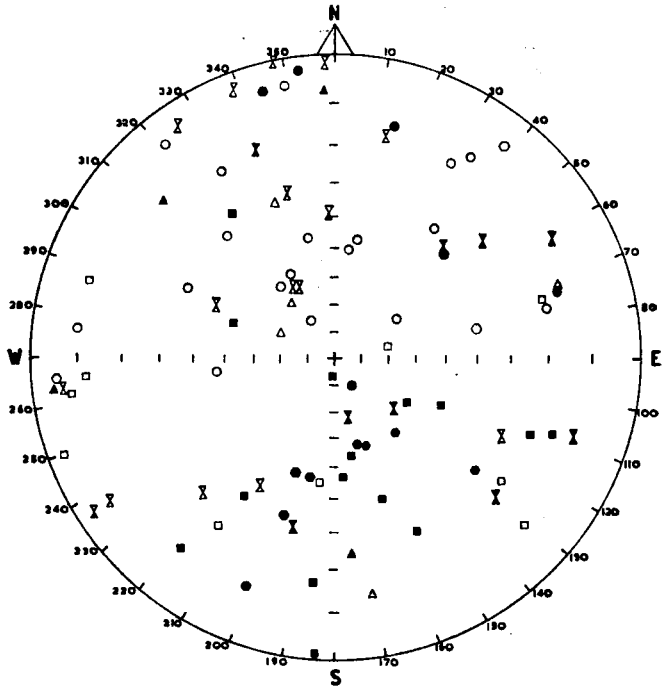

FIG. 5. *Zapala Area.* Uncleaned NRM directions of specimen cylinders of rock.

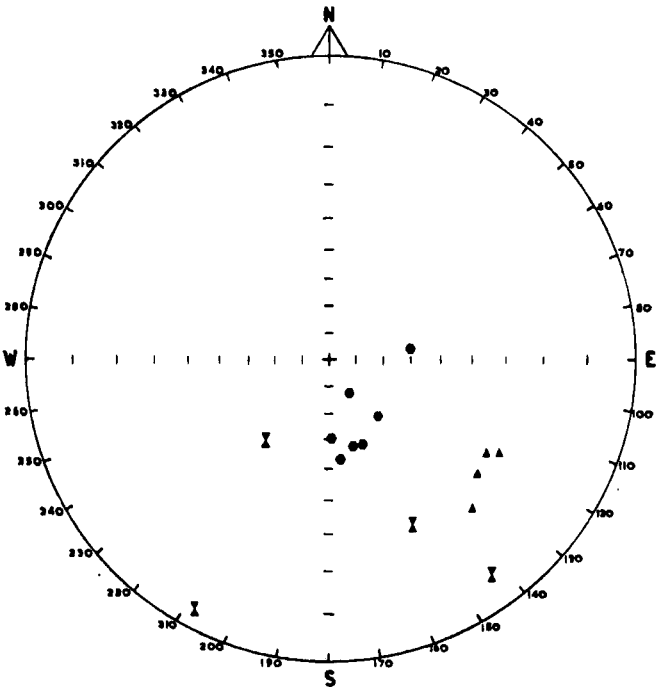

FIG. 6. *South Zapala Area.* Uncleaned NRM directions of specimen cylinders of rock.

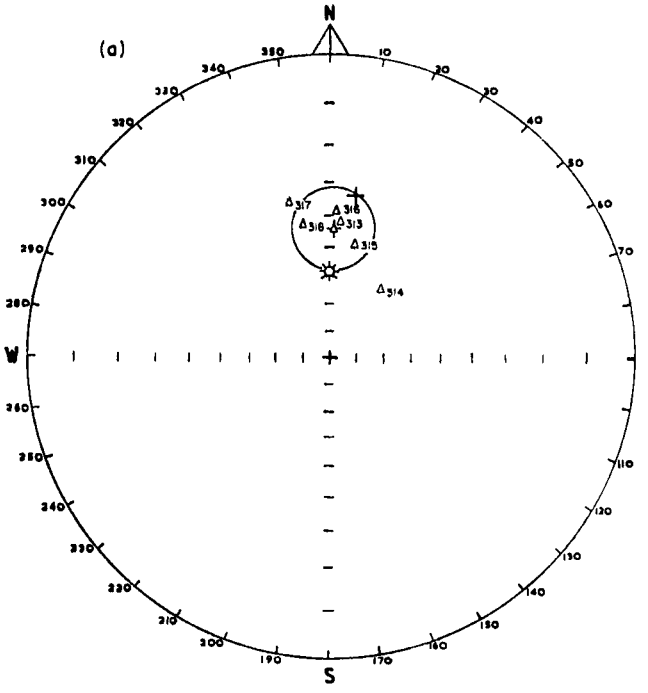

FIG. 7. *Llancanelo Area.* Directions of cleaned remanent magnetization of hand samples: (a) of Basalt III, (b) of Basalt IV, (c) of Basalt V, and (d) of Basalt VII. The mean direction and the 95 per cent circle of confidence is shown for each group.

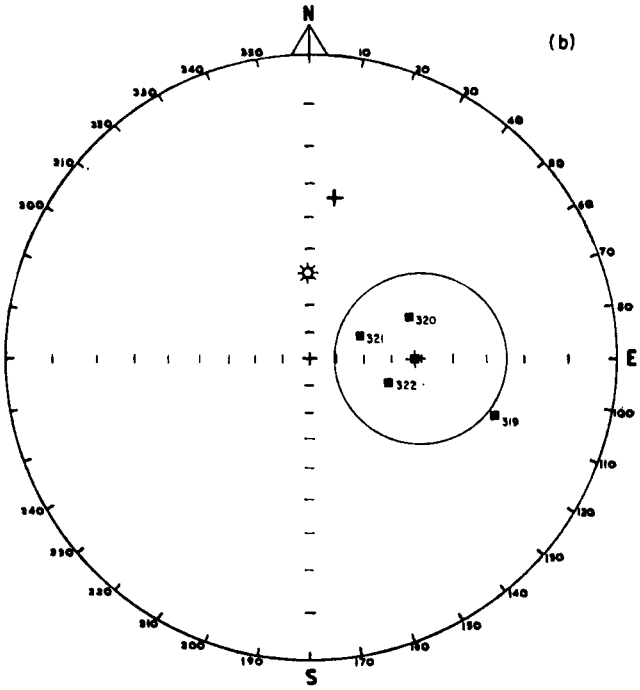

Fig. 7 (b)

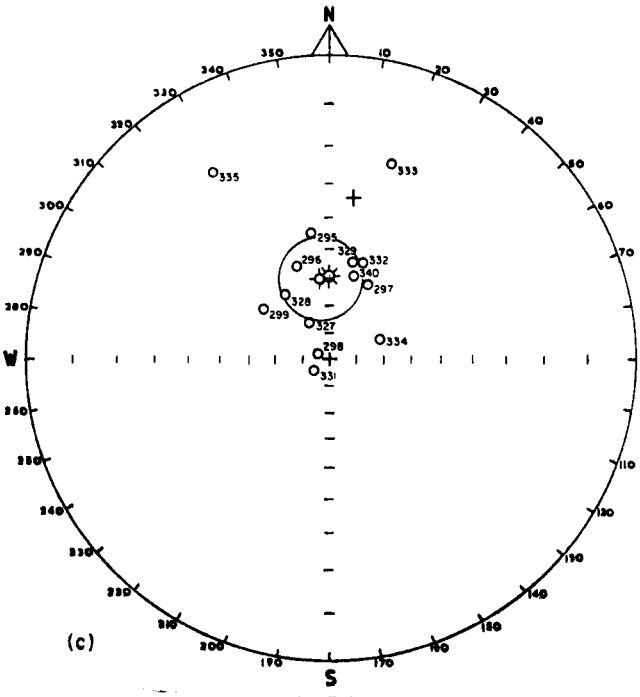

Fig. 7 (c)

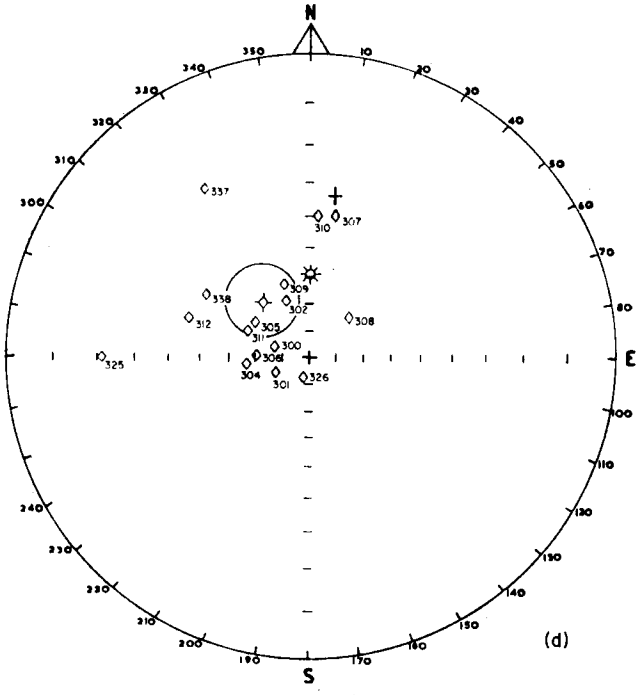

Fig. 7 (d)

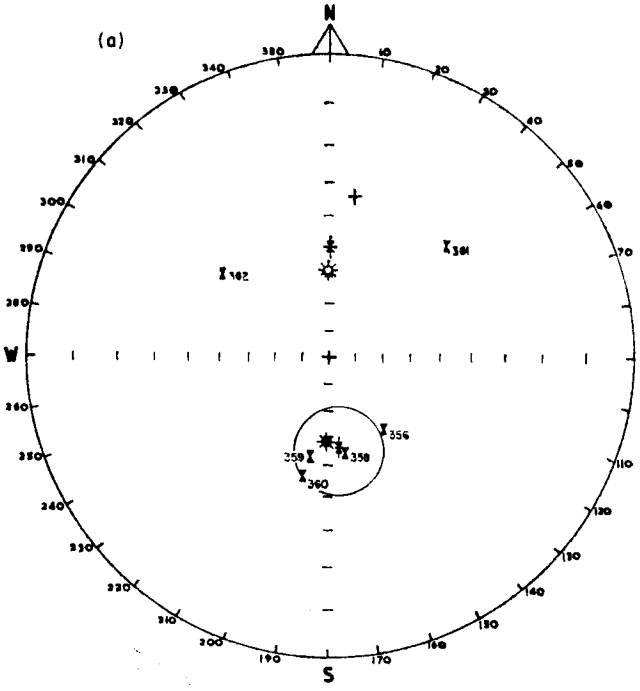

FIG. 8. *Los Volcanes Area.* Directions of cleaned remanent magnetization of hand samples: (a) of Basalt I, (b) of Basalt III, (c) of Basalt IV, (d) of Basalt V, and (e) of Basalt VI.

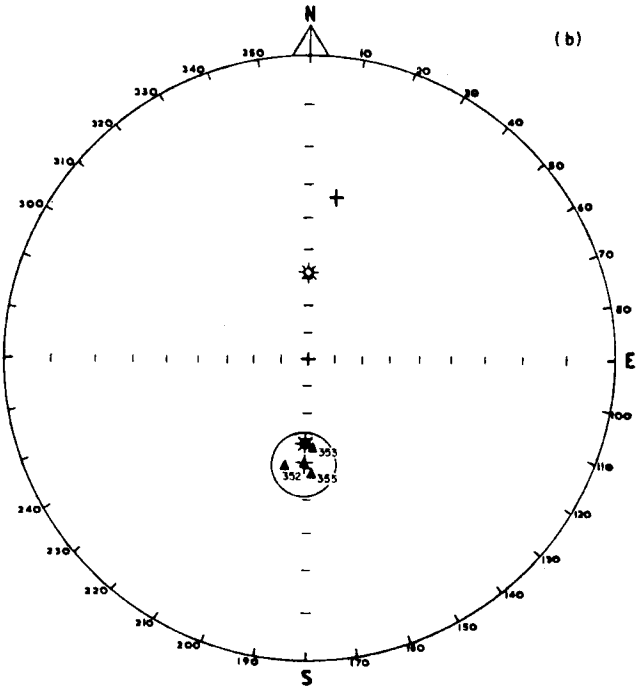

Fig. 8 (b)

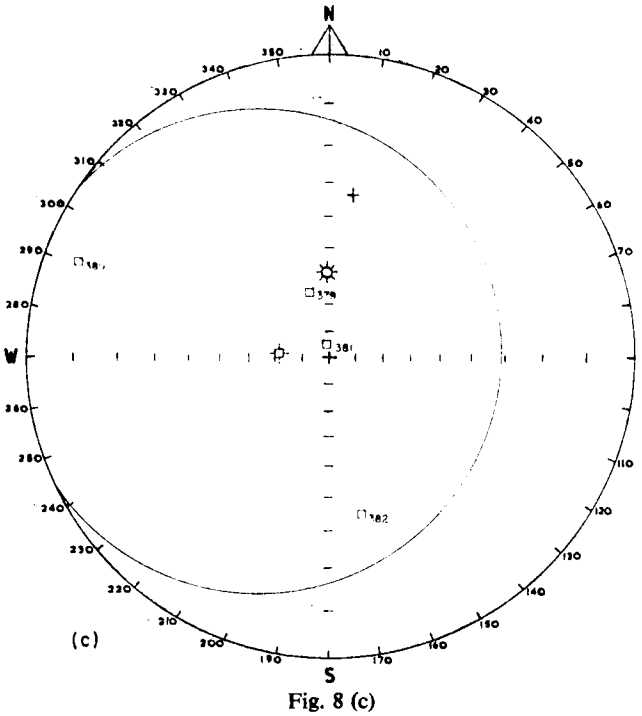

Fig. 8 (c)

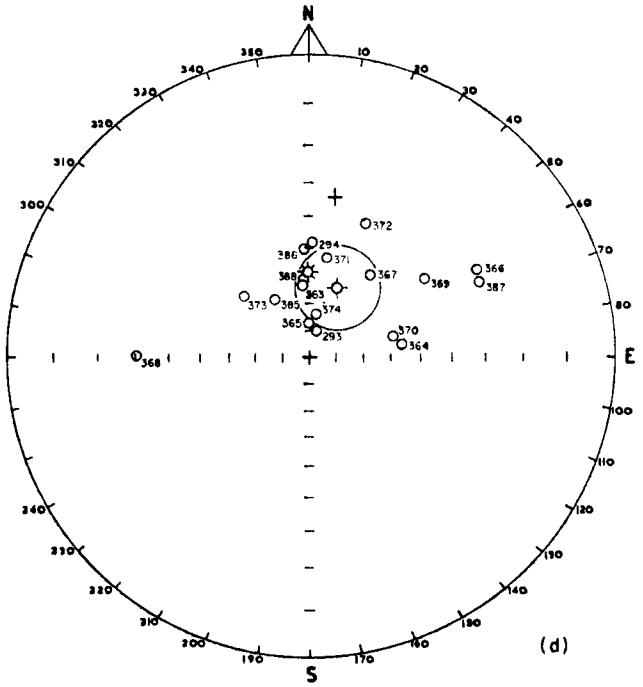

Fig. 8 (d)

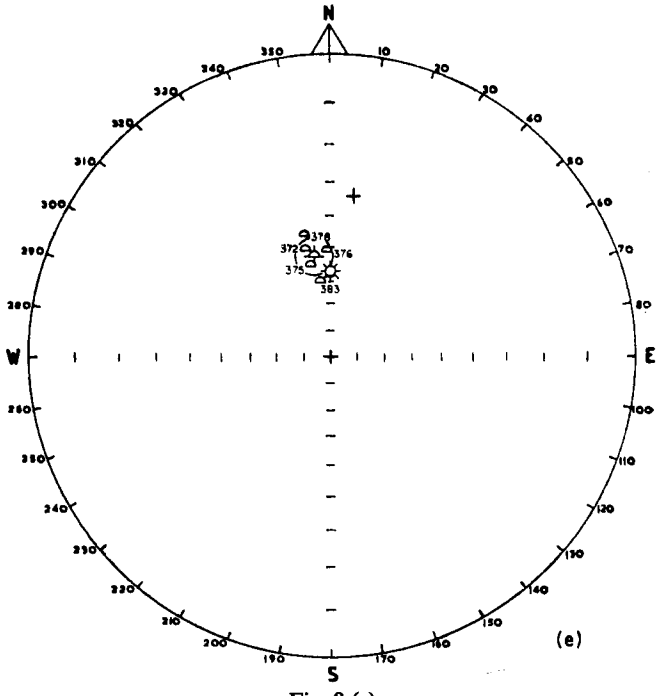

Fig. 8 (e)

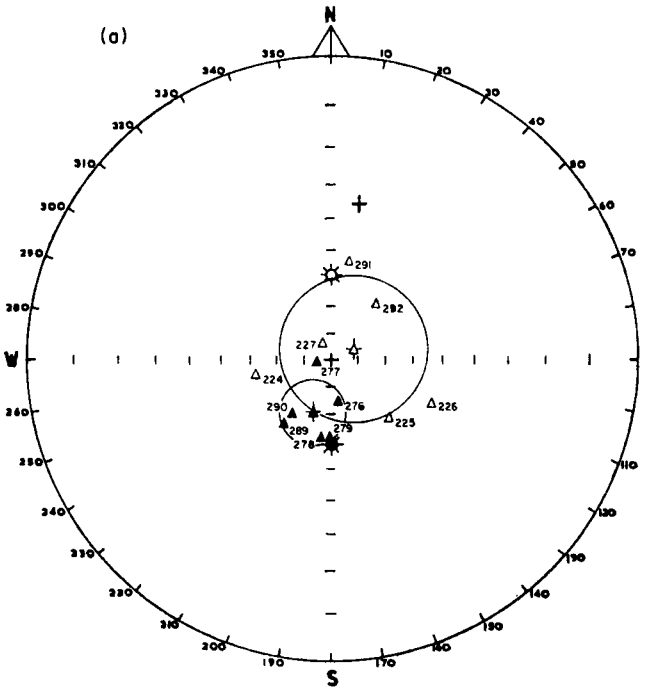

FIG. 9. *Buta Ranquil Area.* Directions of cleaned remanent magnetization of hand samples: (a) of Basalt III, (b) of Basalt IV, and (c) of Basalt V.

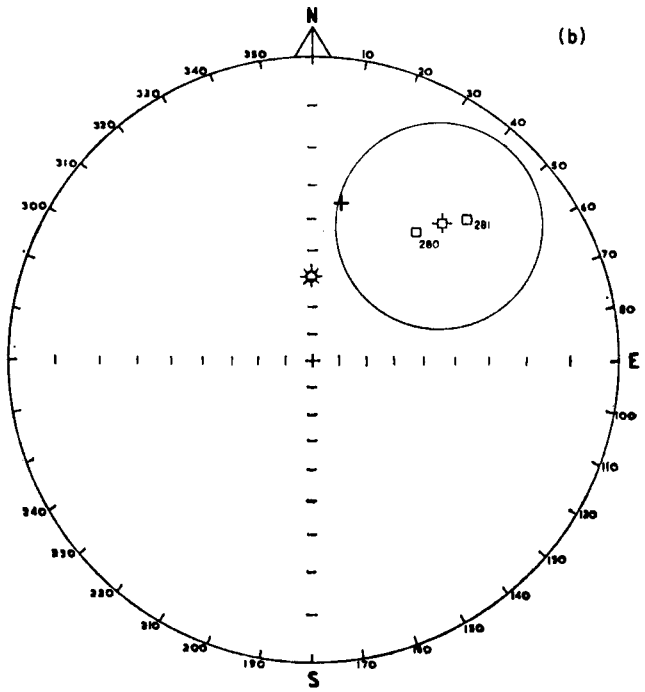

Fig. 9 (b)

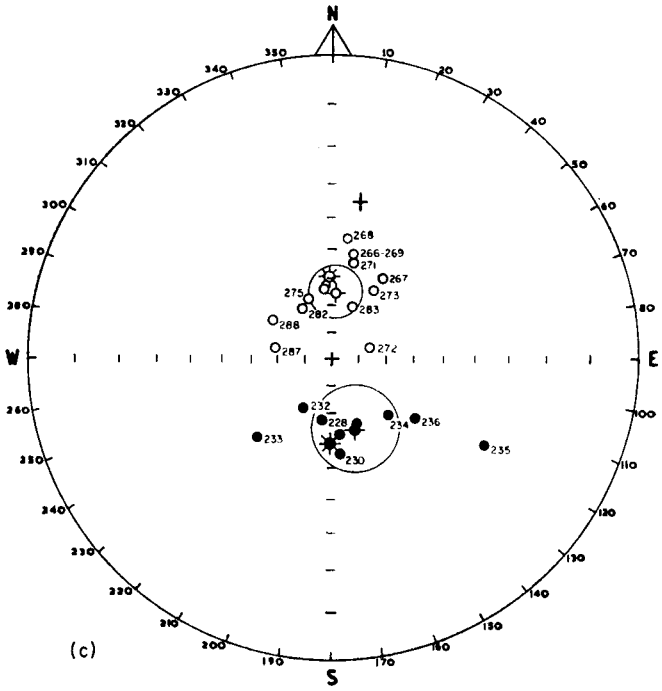

Fig. 9 (c)

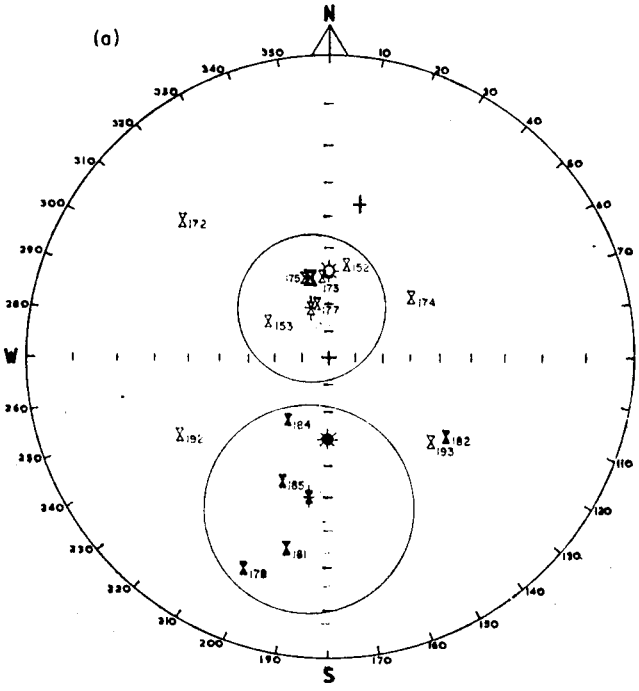

FIG. 10. *Zapala Area.* Directions of cleaned remanent magnetization of hand samples: (a) of Basalt I, (b) of Basalt II, (c) of Basalt III, (d) of Basalt IV, and (e) of Basalt V.

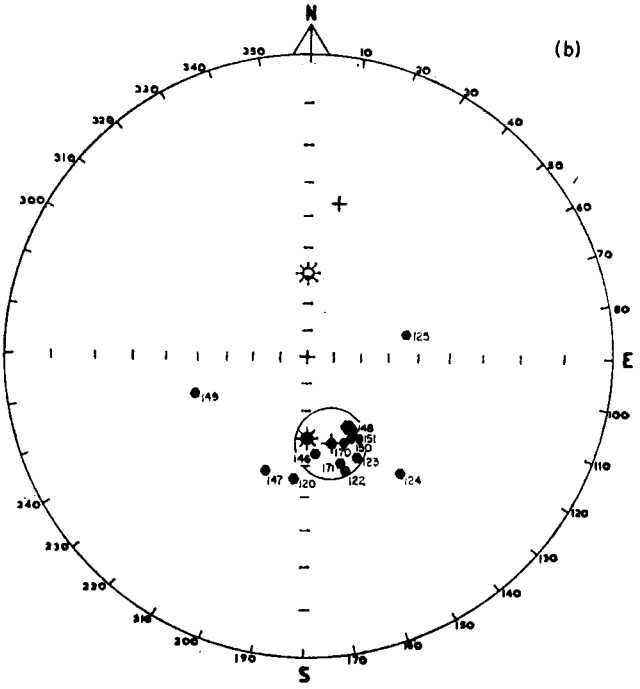

Fig. 10 (b)

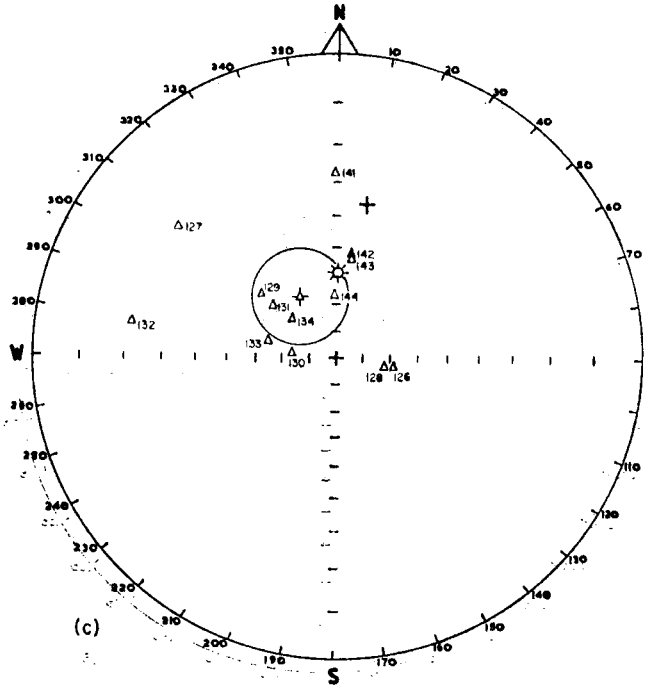

Fig. 10 (c)

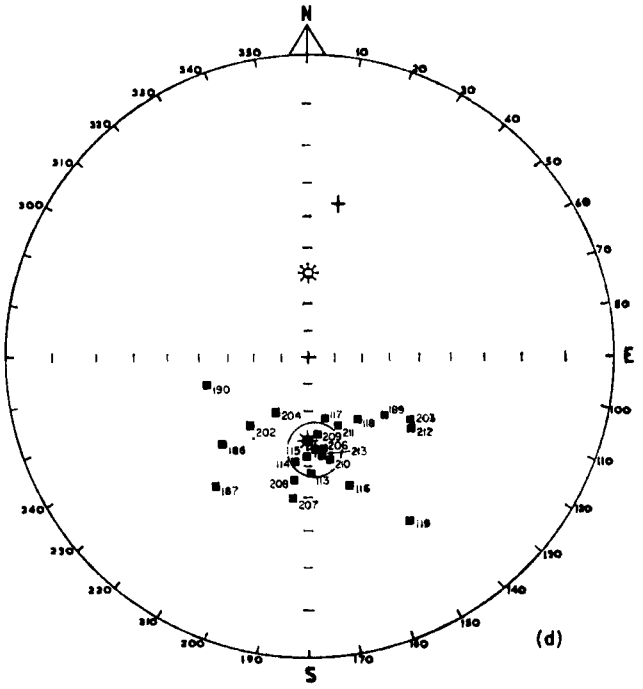

Fig. 10 (d)

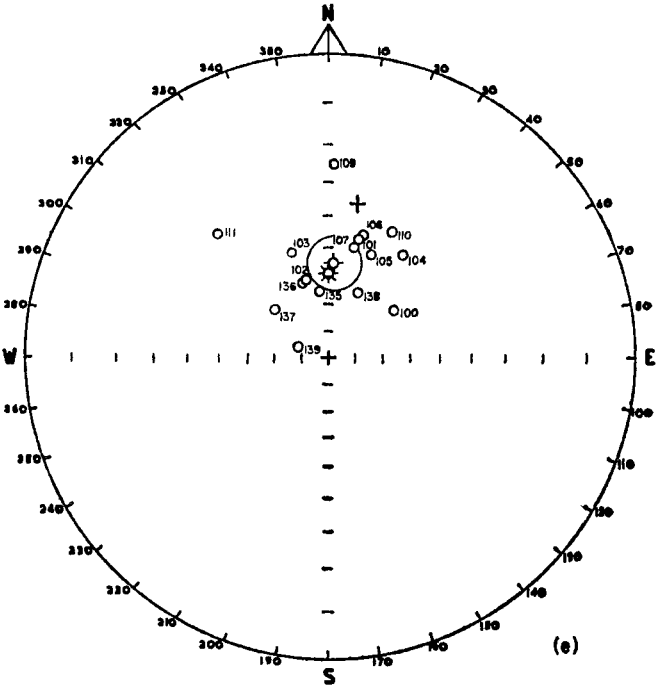

Fig. 10 (e)

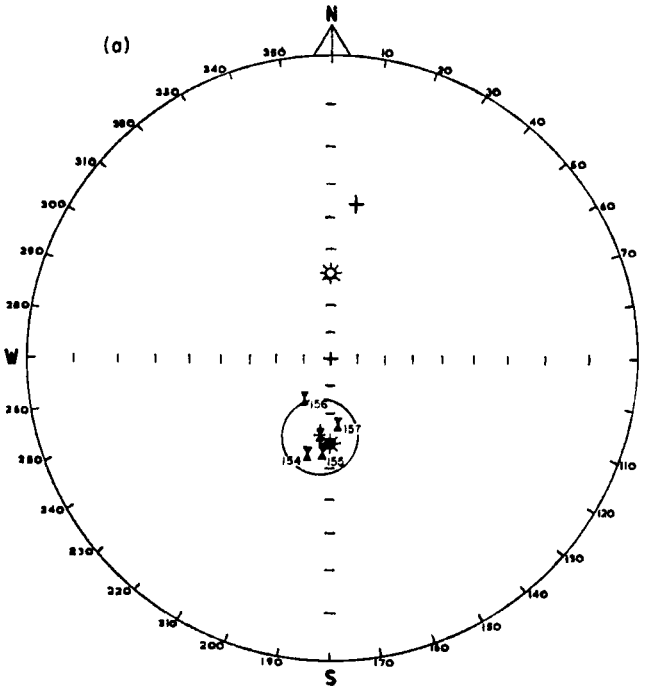

FIG. 11. *South Zapala Area.* Direction of cleaned remanent magnetization of hand samples: (a) of Basalt I, (b) of Basalt II, and (c) of Basalt III.

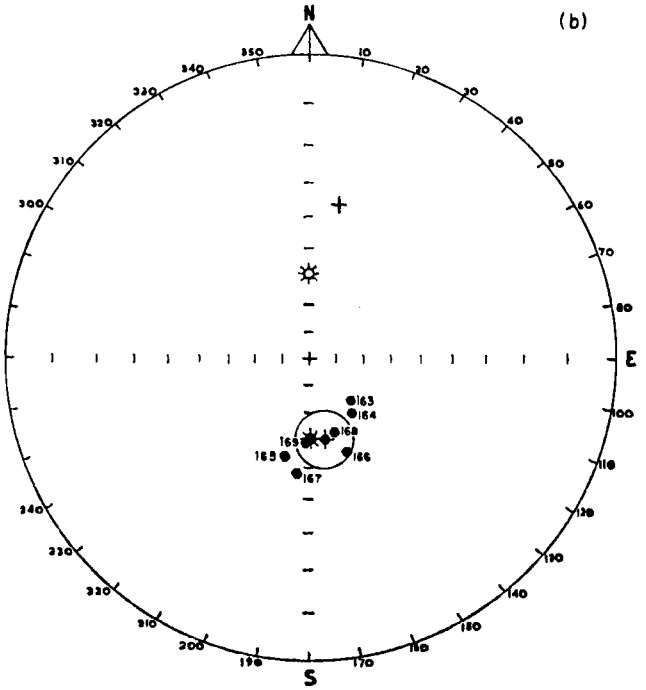

Fig. 11 (b)

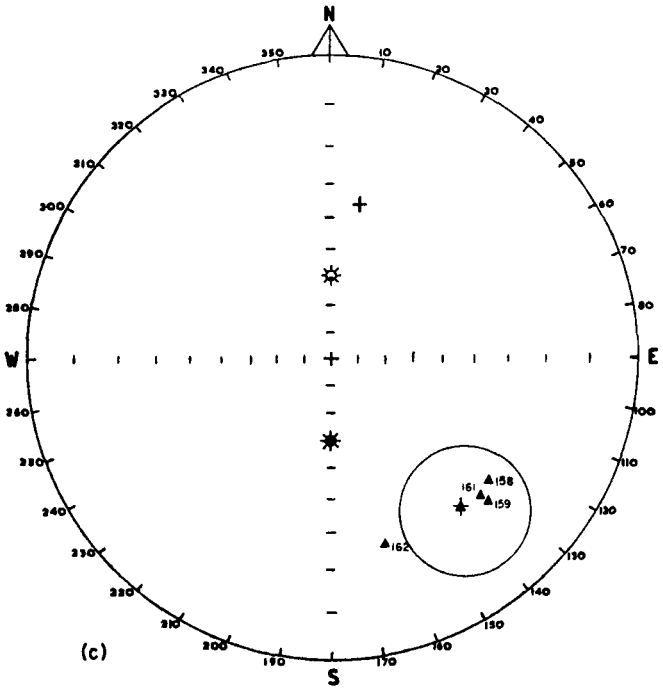

Fig. 11 (c)

This mean direction is different from that for Basalt IV from the Llancanelo area. See Figs 3 and 8.

3.3. *Buta Ranquil area*

Basalts III and V from this area exhibit both normal and reversed polarities of magnetization. The Basalt V flows from the vicinity of Buta Ranquil village have normal polarity whilst those from the vicinity of Tricao Malal have reversed polarity. As in the previous two localities, the polarity of Basalt IV is transitional, nearer to normal than reversed. See Figs 4 and 9.

3.4. *Zapala*

Basalt I exhibits both normal and reversed polarities. Basalt II flows are reversed Basalt IV flows are reversed and Basalt V normal. See Figs 5 and 10.

3.5. *South Zapala*

Basalts I and II exhibit reversed polarity while that of Basalt III is transitional. See Figs 6 and 11.

4. Analysis of palaeomagnetic results

The geomagnetic field was basically of axial dipole character during the time of extrusion of these flows. Nevertheless, in all the areas studied, except Zapala, there exist some basalt flows whose TRM directions differ significantly from the axial dipole field. We suppose that these must have been extruded while the geomagnetic field was in the process of reversing.

Our palaeomagnetic study suggests that certain revisions of the stratigraphy of these Basalts may be necessary.

(i) In the Los Volcanes area, the Basalt III flows have reversed polarity while those from the Llancanelo area have normal polarity. Thus we argue that the effusion of Basalt III at Llancanelo was not contemporaneous with that at Los Volcanes.

(ii) We have also deduced that the Basalt IV from Llancanelo was not contemporaneous with that from Los Volcanes because their cleaned directions of NRM differ significantly. These directions, being non-dipolar, suggest extrusion during a time interval of transition in polarity of the geomagnetic field.

(iii) In the Buta Ranquil area, the Basalt V from Tricao Malal (reversed, axial-dipolar) cannot be contemporaneous with the Basalt V from nearby Buta Ranquil city (normal, axial-dipolar). The same can be said of the Basalt III flows from this area: normal and reversed polarities are encountered.

(iv) Apart from the above anomalies, we have assigned the following magnetic ages to the basalts studied. In the Llancanelo, Los Volcanes and Zapala areas, Basalts V, VI and VII must belong to the Brunhes epoch. Basalt III of the Los Volcanes area could belong to either of the normal events within the Matuyama epoch and Basalt IV to the time when the geomagnetic field was reversing at either the beginning or end of one of the events.

The validity of these age groupings has been borne out by radiometric age determinations by the K–Ar method on this formation of basalts. The results are described in the following paper (Valencio *et al.* 1969).

We may now summarize the palaeomagnetic results from these Quaternary and Tertiary basalts by subdividing them according to the geomagnetic epoch to which we have assigned them. A two-tier analysis (Watson & Irving 1957) has been carried out and the mean directions and statistical parameters are given in Table 3. It is noted that the within-flow dispersions are higher than the between-flow dispersions. This is to some extent due to the occurrence of low temperature oxidation in these basalts and to weathering, which have produced secondary magnetizations. These are not always completely removed in individual specimens by cleaning.

Table 3

Mean directions of cleaned remanence of Argentine basalts

Polarity Epoch or Age	Basalt No.	B	N	D	I	δ	α	δ_w	δ_b
Brunhes	VII, VI and V	6	86	358°	−60°	11°	9°	16°	10°
Matuyama	III	5	28	4°	−60°	19°	18°	18°	17°
Brunhes+Matuyama	VII, VI, V and III	11	114	0°	−60°	14°	8°	17°	13°
Tertiary	II and I	7	44	356°	−57°	11°	9°	25°	6°
Quaternary and Tertiary	VII, VI, V, III, II and I	18	158	359°	−59°	13°	6°	20°	11°

Notes: Two-tier analysis carried out:

B = No. flows,

N = No. samples,

δ = circular SD including within and between lava dispersion,

δ_w = average within lava dispersion,

δ_b = between lava dispersion,

α = 95 per cent circle of confidence.

Table 4

Virtual north poles calculated from Argentine basalts

	Long (°E)	Lat (°N)	δ (°)	α(°)	δ_b (°)
Brunhes	131	85	17	14	16
Matuyama	75	85	27	27	26
Brunhes + Matuyama	106	85	21	12	20
Tertiary	194	86	13	10	9
Quaternary + Tertiary	132	87	18	8	17

Notes: Symbols have same meaning as in Table III.

Furthermore only a weak relict of the primary TRM may remain so the precision of measurement is less than it would be for stronger primary components. We are satisfied, however, that the errors resulting from the above causes are random and not systematic.

In Table 4, mean positions of the virtual poles corresponding to the mean directions listed in Table 3 are given. None of these differs significantly from the present geographic pole, populations having been made up of virtual north poles for normal epochs such as the Brunhes epoch and of virtual south poles for reversed epochs such as the Matuyama.

5. Palaeosecular variation

The possibility of investigating the ancient secular variations of the geomagnetic field by palaeomagnetic studies has been discussed by a few authors, e.g. Creer (1962). More recently Creer & Sanver (1968) described an analysis for this purpose of the then available palaeomagnetic data for Quaternary and Tertiary basalts from all over the world and the results for the Neuquén basalts are included in their Table 1.

The basalts have been grouped according to age as indicated in Table 3 and a two-tier statistical analysis (Watson & Irving 1957) has been applied as described in Section 4. In the first tier the mean vector for each sample (total N) is treated as a unit and in the second tier the mean vector for each flow (total B) is assigned unit weight. (Note, the term sample refers to a hand sample which is cut into several cylindrical specimens to be measured.)

The between-lava flow dispersion is taken to have been produced by palaeosecular variations of the geomagnetic field, and values of 10°, 17° respectively are found for the Bruhnes and Matuyama epochs. Combining the data for these two epochs the between-flow dispersion is 13° (Table 3).

In order to compare these with data from other places it is necessary to correct them for latitude to the value we should expect at the equator. This may be done if one supposes that, on average, the intensity of the non-dipole field is independent of

Table 5

Polarity Epoch	Between-flow C.S.D. Neuquén flows	Between-flow C.S.D. World average	Mean Perturbing Field h/H Neuquén flows	Mean Perturbing Field h/H World average
Brunhes	15°·2	18°·2	0·33	0·39 ± 0·09
Matuyama	24°·9	20°·6	0·53	0·44 ± 0·13
Br + My combined	19°·3	18°·8	0·41	0·40 ± 0·10
1945 Model Field		18°·5		0·40 ± 0·01

latitude. We know the dipole field intensity depends on latitude following $(1+3\sin^2 L)^{\frac{1}{2}}$, so $\delta_0 = \delta_L\ (1+3\sin^2 L)^{\frac{1}{2}}$. This correlation has been applied in compiling Table 5. We may compare the values obtained, viz. 15°, 25° and 19° for the Brunhes, Matuyama and for these two epochs combined with the average values for world wide data of 18°, 21° and 19° respectively (see Table 2 of Creer & Sanver 1968). Furthermore the theoretical value, computed for a model field whose time variation is represented by rotating the observed 1945 field about the geographic axis, is 18°·5 (Creer 1962).

Alternatively we may represent the secular variation field by a randomly directed perturbing field of equal magnitude h over the globe superimposed on an axial dipole field of strength H at the equator (Irving & Ward 1964). Adopting this model we have computed values for h/H for the Neuquén lavas and we compare them with the world average values in Table 5.

Thus we think it reasonable to conclude that the between flow dispersion does in fact reflect the palaeosecular variations of the geomagnetic field.

6. Compositional and experimental Curie points

6.1. *Homogeneous titanomagnetites*

Electron microprobe analysis shows that in cases where rocks contain homogeneous titanomagnetites these are invariably rich in titanium so that low Curie points would be expected. Analyses of several samples are listed in Table 6. The composition is expressed as x in the formula $(1-x)\,Fe_3O_4 + Fe_2TiO_4$. In deducing '$x$', allowance for the trace elements is made by adding them to the iron, expressing them as weight per cent of equivalent iron (Creer & Ibbetson 1969). This is justified since the trace elements are divalent or trivalent and are thus not to be expected to replace titanium which is quadrivalent. The Curie points appropriate to the x values deduced from the microprobe analyses have been deduced assuming a linear variation between 575 °C for $x = 0$ and −120 °C for $x = 1$. In fact we should expect the Curie points of the natural titanomagnetites to be a little less than these values due to the effect of the trace elements, which can be estimated from the work of Frohlich, Löffler & Stiller (1965). Creer and Ibbetson (1969) have observed that

Table 6

Microprobe and petrological data

Basalt No.	Sample No.	x	T_p	T_0		Type of $J_s(T)$ curve	Degree of oxidation	Grain size (μm)
I	152	0·70	85° C	100°	530° C	2	2	100
III	289	0·75	30°		575°	4	4	10, 70
III	317	0·52	210°		550°	3–4	4	10–20
IV	115	0·72	70°		530°	4	5	20
IV	117	0·68	65°	300°	540°	2	2	20
IV	118	0·74	25°		520°	4	3	60
IV	203	0·51	220°	225°	500°	2	2	10–30
IV	376	0·61	150°	130°		1	1	20–30
V	139	0·51	220°	190°	450°	2	1	30–40
V	293	0·61	150°	150°		1	1	20–30

x refers to composition in series $(1-x)\,Fe_2O_3 . xFe_2TiO_4$.

T_p is the compositional Curie point deduced from x,

$J_s(T)$ curves are shown in Fig. 12.

T_0 are the measured Curie points.

the measured Curie points of rocks which contain homogeneous titanomagnetites are invariably low and in good agreement with those deduced from microprobe analysis. Examples of such basalts containing such unoxidized and optically homogeneous titanomagnetites are samples 293 and 376 (Fig. 12b and c). We shall identify such $J_s(T)$ curves by referring to them as type 1 curves.

Sometimes the Curie temperatures of basalts containing optically homogeneous titanomagnetites have been found to be higher than the values expected for the compositions determined by the microprobe. Examples of such rocks are samples 152 (Fig. 12a), 117 and 203 (Fig. 12b) and 139 (Fig. 12c) and thermomagnetic curves of this shape, where two Curie points can be distinguished will be referred to in this paper as type 2. We have noted that such samples usually come from the surface of the flows. It has been argued that thermomagnetic curves of this type are characteristic of oxidized titanomagnetite (Creer & Petersen 1969), and these authors have concluded that a submicroscopic intergrowth exists in these titanomagnetites although they appear optically homogeneous.

6.2. *Exsolved titanomagnetites*

Whenever exsolution was observed, even if only to a very minor extent, along cracks or around rims, Curie points of about 500 °C are measured. In cases where exsolution is slight, or where unexsolved grains coexist with exsolved ones two Curie points are exhibited and the curves are like type 2 (see Section 6.1). When exsolved grains predominate, type 4 type curves are found, examples being those for samples 289 and 317 (Fig. 12a), 115 and 118 (Fig. 12b). In addition it is convenient to define a type of curve whose shape is between those of type 2 and type 4 curves. We shall name these curves, type 3, and here the magnetization decreases almost linearly with temperature down to the Curie point.

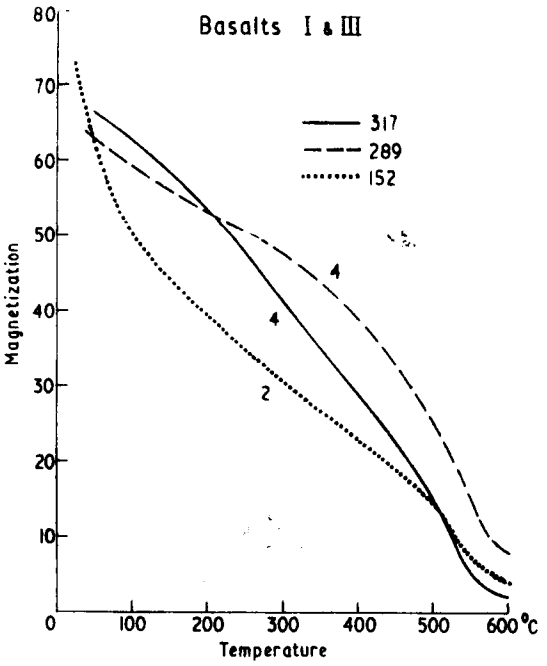

FIGS (12a), (b), (c). Examples of thermomagnetic curves, of types 1, 2, 3 and 4 as defined in text.

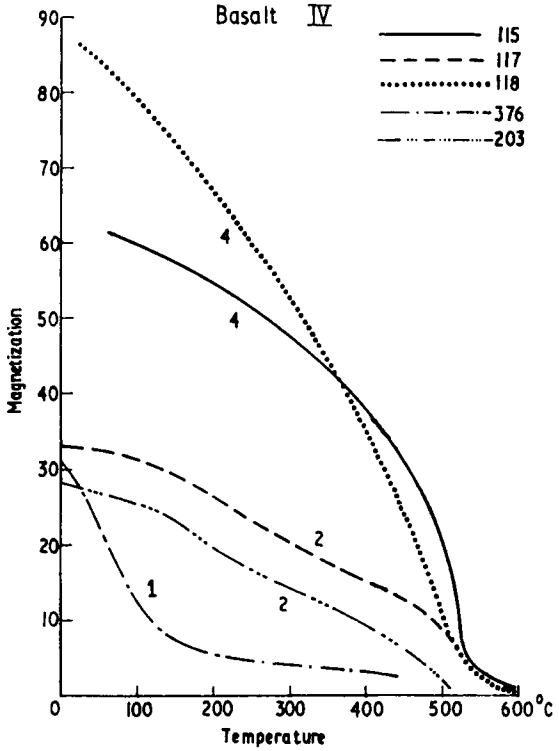

Fig. 12 (b)

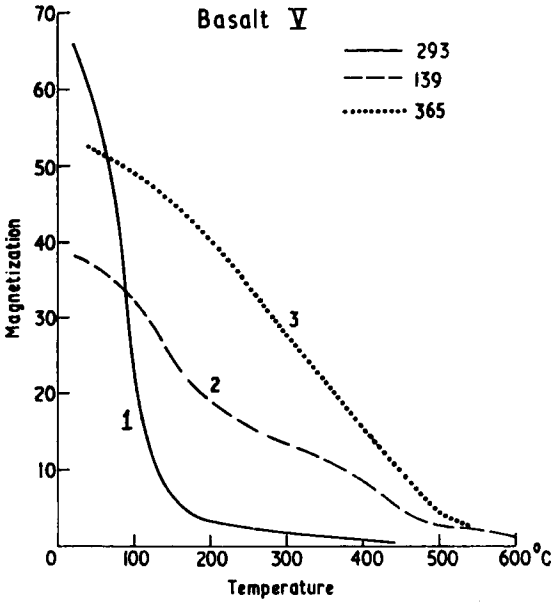

Fig. 12 (c)

In Table 7 we list thermomagnetic data for 25 specimens of different oxidation stage. Oxidation stage 1 exhibits either both a low and high Curie point or only a low one. Oxidation stage 2 usually exhibits two Curie points or only a high one. Basalts of oxidation stages 3 and 4 usually exhibit only a high Curie point, but in a few rocks where the amount of oxidation is variable, a low Curie point may sometimes also be observed.

The exsolved regions are often of the order of a micron across and thus are too small to be analysed accurately with the microprobe. When the beam is rastered over an area of about 50 square microns so as to measure the average composition, this is typically found to be rich in Ti as for the homogeneous titanomagnetites.

7. On the possibility of low temperature oxidation

As already stated in Section 6, the presence of two Curie temperatures in basalts containing homogeneous titanomagnetites (type 2 $J_s(T)$ curves) may be taken to indicate the occurrence of oxidation in these rocks at ambient temperatures, for, as Creer & Petersen (1969) have argued, exsolution on a submicroscopic scale of an iron rich spinel phase may have occurred in the titanomagnetites in these rocks. As distinct from this process, we now consider the effects of surface weathering.

Table 7

Oxidation stage and Curie points

Oxidation stage	Basalt No.	Area	Sample No.	Grain size (μm)	TM curve type	Curie points (°C)	
1	V	BR	274	10	1–2	150	520
1	V	LV	385	30	1	100	
2	IV	Z	113	60	2	150	520
2	IV	Z	117	20	4		550
2	I	Z	152	100	2	150	525
2	IV	Z	203	10–30	2	220	530
2	V	BR	232	25	1	200	
2	VII	LL	326	10	2	100	490
2	V	LL	336	10	4		500
2	V	LV	365	10	3–4		510
3	IV	Z	118	60	4		560
3	III	Z	132	50–150	4		570
3	I	SZ	154	20–50	4		510
3	I	Z	184	50	4		555
3	V	BR	229	5, 100	2	220	575
3	III	LL	317	10–20	3–4		530
3	V	LL	335	10, 50	3		515
3	IV	LV	381	30	4		520
4	V	Z	102	2–5	2	220	520
4	III	BR	289	10, 70	4		570
4	V	LL	333	10, 70	4		510
4	I	LV	362	30, 70	4		565
4	V	LV	367	10–20	4		510
5	IV	Z	115	20	4		570
5	II	SZ	163	50–100	4		560

Notes: 1. Areas denoted as follows: LL = Llancanelo, LV = Los Volcanes, BR = Buta Ranquil, Z = Zapala, and SZ = South Zapala.

2. Thermomagnetic curve types are defined in Figs 18a, 18b and 18c.

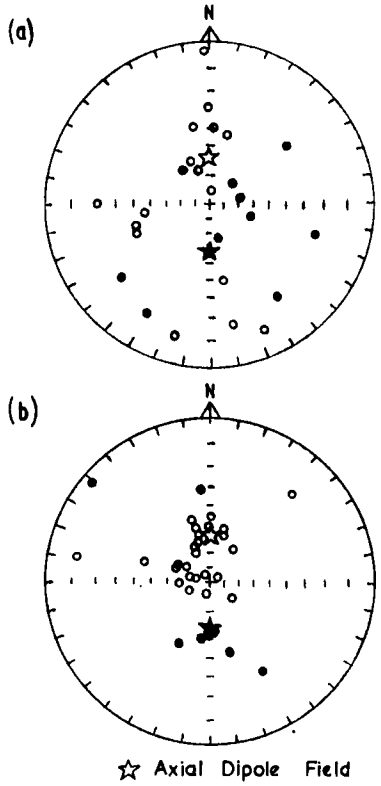

FIG. 13. Typical NRM directions of specimens with intensities (a) greater than 10 milligauss, (b) less than 10 milligauss.

Sanver (1968a) noted a correlation between high NRM intensity and scatter of NRM directions in the Neuquén basalts. The directions of NRM of samples with intensities greater than about 10 milligauss were more highly scattered than in more weakly magnetized rocks as illustrated in Fig. 13. Furthermore, ore microscope studies of polished sections of such rocks revealed the presence of maghemite, which must have been produced by weathering. We would not expect the effects of weathering to have been uniform throughout a formation, and so this might well explain the large differences in NRM intensity sometimes observed between samples from a given site and the different alternating magnetic fields required for cleaning such samples.

In a comparative study, Sanver (1968a) concluded that the NRM intensities of the Argentine basalts were higher than those of Quaternary and Tertiary basalts from Turkey (Sanver 1968b) and from Oregon (Sanver 1968a), the geometric mean intensity of the Argentine basalts (about 20 milligauss) being about two and a half times that of each of the other two collections. The ratio M/M_0, of cleaned to natural intensity was smaller for the Argentine collection than for the others. On the other hand there was no significant difference in the geometric mean susceptibility values for the three collections.

Hand samples both from quarries and from natural exposures were collected of the Turkish basalts. Both hand samples and 6 in. cores of 1 in. diameter of the Neuquén basalts were sampled principally from natural exposures, while all samples from the Oregon basalts were drilled. The average degree of oxidation (Wilson & Watkins 1967) of the Turkish basalts was less than that in the Neuquén basalts and

also there was less indication of oxidation at ambient temperatures. The Oregon basalts were invariably highly exsolved. Electron microprobe analyses of homogeneous titanomagnetite grains samples of the Argentine and Turkish basalts (there were no such grains in the Oregon collection) indicated that the former contained more Ti (see Creer & Ibbetson 1969).

It is not clear which of the above differences is responsible for the higher degree of ambient temperature oxidation (i.e. within class 1 of the Wilson–Watkins scale) in the Argentine basalts, although it can be stated definitely that the fine scale exsolution discussed by Creer & Petersen (1969) cannot have occurred in the Oregon basalts because they were already exsolved at high temperatures before cooling. It is possible that the climatic conditions in Neuquén and Mendoza provinces of Argentina may have produced more severe weathering than the climate in Anatolia. The methods of collection adopted were similar in both regions in that surface or near surface samples were taken.

While the inclusion of samples which have been subjected to ambient temperature oxidation in a collection could be obviated by drilling sample cores from depth, sensible palaeomagnetic results can now nevertheless be obtained from near surface samples, provided rock obviously subjected to heavy weathering is avoided. It is a matter of balancing the extra time spent in collecting deep-drilled cores against the extra time spent in cleaning partially remagnetized hand samples in the laboratory. The latter samples, however, present many interesting problems in rock magnetism and for this reason alone they are well worth while studying.

Table 8

Basalt No.	Sample No.	Titano magnetites size (μm)	Degree of oxidation	A.F. coercivity (Oe)	NRM intensity (mG)	$M_{150°}/M$	Blockage Temperature (°C)	Curie Temperature (°C)	Polarity
II	123	10	3	450	3	1·10	400–570	570	*R*
	124	10–20	2	150	83	0·02	0–520	520	*R*
II	146	30	3	550	34	0·77	200–570	570	*R*
	147	30	2	120	178	0·32	400–520	520	*R*
II	163	30	5	500	32	0·90	200–520	570	*R*
	169	40	4	120	184	0·54			*R*
III	222	55	2	520	44	0·83	130–250	250, 520	*N*
	224	75	1	150	367	0·59	~130		*N*
III	316	30	3	500	117	0·71	400–420	520	*N*
	313	55	2	200	103	0·58	130–250	250, 520	*N*
III	355	50	3	350	24	1·00	400–570	570	*R*
	353	55	3	120	94	0·68	130–520	520	*R*
V	210	20	2	350	3	0·90	200–400	400	*R*
	207	25	1	150	37	0·16	~150		*R*
V	231	25	2	300	66	0·87	400–520	520	*R*
	236	30	2	150	65	0·20	0–300	300	*R*
V	269	10	3	500	45	1·00	400–520	520	*N*
	268	20	3	180	37	0·35	200–400	520	*N*
V	371	25	3	470	91	0·87	0–400	400	*N*
	369	30	2	150	180	0·11			*N*

8. On the relationship between the various magnetic and petrological properties

8.1. *Differences between stable and unstable specimens*

It was noted that the remanence of different samples from the same flow sometimes showed different response to treatment by alternating magnetic fields during cleaning. An attempt was made to investigate the reasons for this in the following manner. Pairs of samples from the same flow, one showing a markedly higher stability than the other, were selected from ten different flows. The coercivities, H_{cb} as defined in Section 2, are listed in column 5 of Table 8. The mean size of titanomagnetite grains and the degree of oxidation (Wilson & Watkins (1967) scale) are listed in columns 3 and 4. Within each pair, there seems to be a tendency for the sample with the higher A.F. coercivity to have the higher oxidation number, this being so for 8 out of the 10 pairs. In the other two pairs the oxidation numbers are equal, and one of these pairs has normal and the other reversed polarity. NRM intensities are listed in column 6, where it may be observed that for 7 out of the 10 pairs, the intensity of the sample with the lower coercivity is higher than that of the sample with the higher coercivity, in some cases markedly so. The ratios between intensity after cleaning in an A.F. of peak value 150 oersteds, and the NRM are listed in column 7. In columns 8 and 9 are listed the blockage temperatures of the NRM and the Curie temperatures respectively. There is a tendency within pairs of samples, for the blockage temperatures of the ones with the lower A.F. coercivity to be lower than those of the ones with the higher coercivity. The Curie points are mainly in the 520°–570° range with an additional low Curie point in some of the samples which are of oxidation degree 2.

8.2. *Polarity, the degree of oxidation and intensity*

There seems to be no obvious difference in properties of normally and reversely magnetized samples. There is no correlation between polarity and oxidation number as shown in Table 9 below.

In the limited number of specimens studied and summarized in Table 8 there does seem to be a significant difference between the average intensity of NRM of normal and reversely magnetized samples, as may be seen in Table 10 below. Geometric mean intensities are given. In brackets are given these mean intensities raised or lowered by the standard error as appropriate. It should be noted that secondary components of magnetization produced by the present geomagnetic field

Table 9

Numbers of specimens listed in Table 8 *having N or R polarity within each oxidation class*

	Degree of oxidation				
Polarities	1	2	3	4	5
N	1	3	4	0	0
R	1	5	4	1	1

Table 10

	Geometric mean intensity of NRM (milligauss)	
Polarities	Stable member of pair	Unstable member of pair
N	68 (50)	126 (76)
R	13 (24)	91 (118)

must have normal polarity and hence when present will increase the intensity of NRM of samples with normally polarized remanences. It is interesting to note that the difference between the intensities of normal and reversed 'stable' samples (i.e. those with harder secondary magnetizations as indicated by higher A.F. coercivities) is significant at the level of probability (63 per cent) appropriate to the standard errors: the G.M. intensity minus the SE of the normal group is 50 mG while the G.M. intensity plus the SE of the reversed group is only 24 mG. The difference between those of the unstable members of each pair (i.e. those with less hard secondary magnetizations) is not significant at this level of probability: the G.M. intensity of the normal group minus the SE is 76 mG while that of the reversed group plus the SE is 118 mG and this overlaps the former (see Table 10).

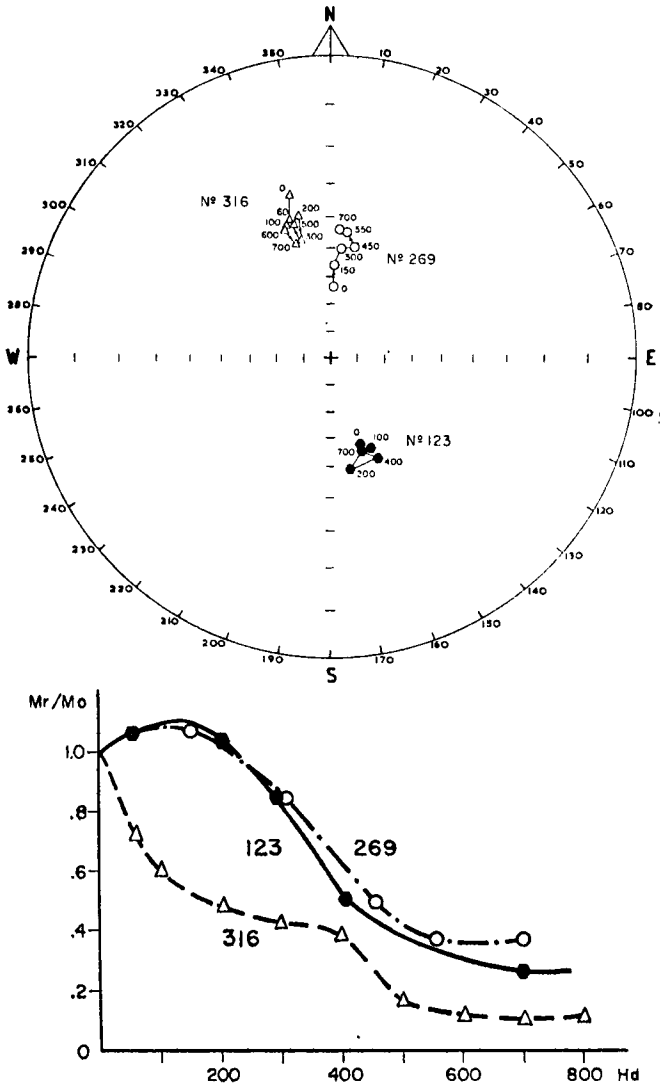

FIG. 14. To illustrate the presence of stable (a) and unstable (b) samples in the same flow. Changes in direction and intensity of specimens in response to A.F. cleaning. Samples 123 and 124 come from Basalt II, 268 and 269 from Basalt V, 313 and 316 from Basalt III.

9. Variation of properties of basalt in time and space

A preliminary attempt has been made to study this by calculating the average values of intensity of remanence and of A.F. coercivity in sets of samples grouped (a) according to age and (b) according to area of collection.

9.1. *Intensity of remanence*

The distribution of intensities is log—normal. Therefore we have computed geometric means rather than arithmetic ones. Mean values for the whole collection of NRM (M_0) and of remanent magnetization after cleaning (M), with their standard errors ($M \pm$ SE) and standard deviations ($M \pm$ SD) are shown in Figs 15 and 16. In Fig. 15 are shown mean values for each flow group and in Fig. 16 mean values for each area of collection. Standard error bars are also shown and it is apparent that the scatter of flow group means is considerably greater than that of area means.

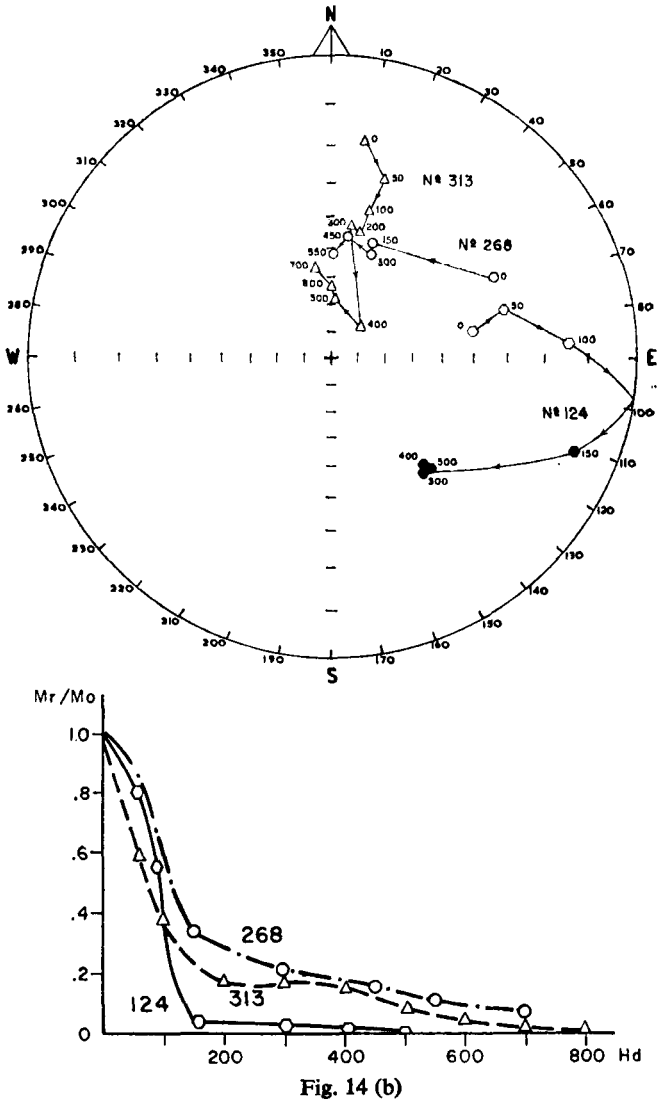

Fig. 14 (b)

In fact, for four out of the five area means, the standard error bars include the overall mean value M and that for the fifth area, Llancanelo, very nearly does.

We conclude tentatively that the intensity of remanence of the basalts varied more with time of extrusion than with geographic area at a given time. But if definite conclusions are to be drawn about this, it will be necessary to study many more samples.

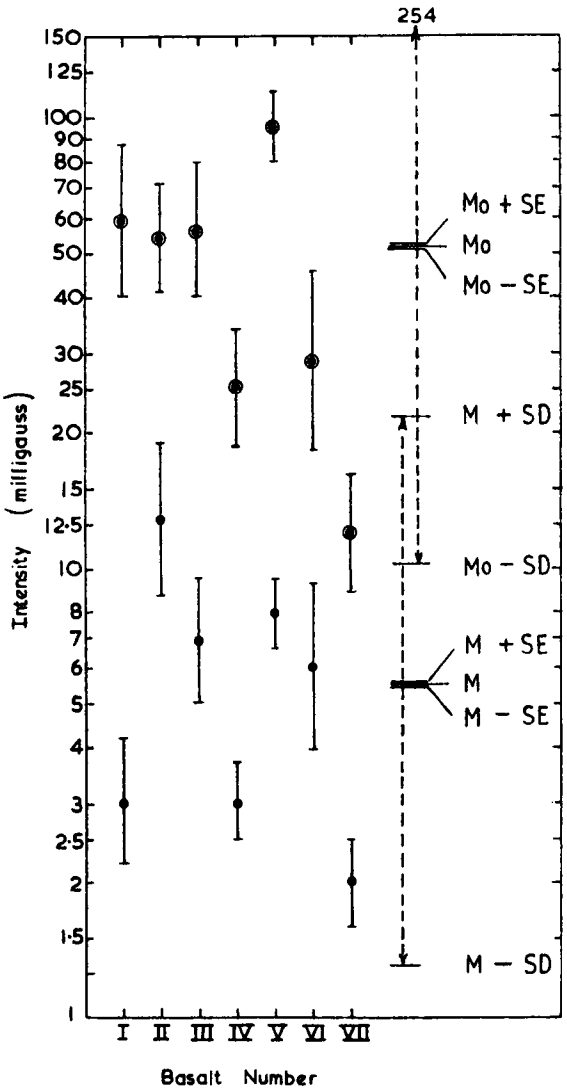

FIG. 15. Geometric mean intensities with standard errors for each group of flows, I to VII. Overall mean with its standard error and standard deviation also shown.

Mean Intensities group by group: ⊙ = initial values, ● = cleaned values. Standard errors shown: *M*, *Mo*: overall means, *M* = cleaned values, *Mo* = initial values, SD = standard deviation, SE = standard error.

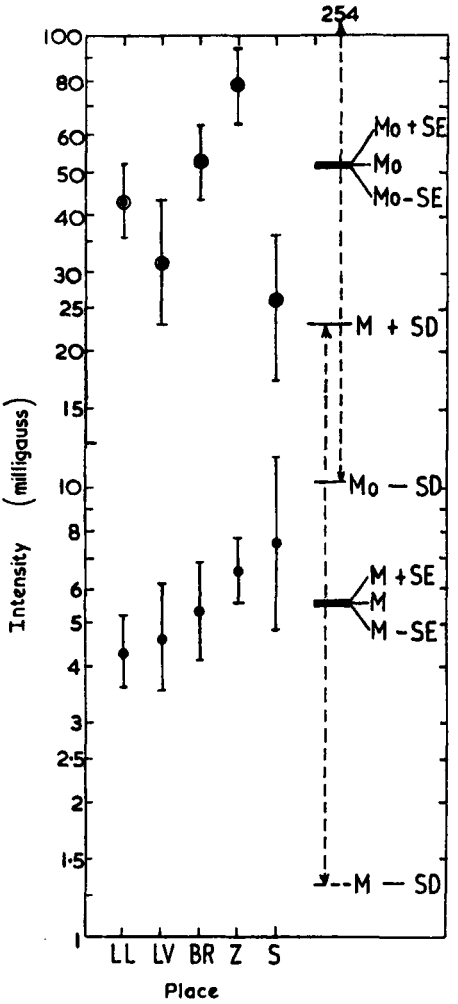

FIG. 16. Geometric mean intensities with standard errors for each of the five areas of collection. Overall mean with its standard error and standard deviation also shown.

Mean Intensities, area by area: ⊙ = initial values, ● = cleaned values. Standard errors shown: *M*, *Mo*: overall means, *M* = cleaned values, *Mo* = initial values, SD = standard deviation, SE = standard error.

9.2. *Critical A.F. values required for cleaning*

Again the distributions are log—normal so that geometric means have been calculated. Means of both the estimates of coercivity, H_{ca} and H_{cb}, defined in Section 2 for each flow group and for each area are illustrated in Fig. 17. Standard error bars are also shown and for the overall means, both standard errors and standard deviations are given.

It is not possible to draw any conclusion about whether or not the A.F. coercivity shows a greater variation with the age of the flow than with the area of collection.

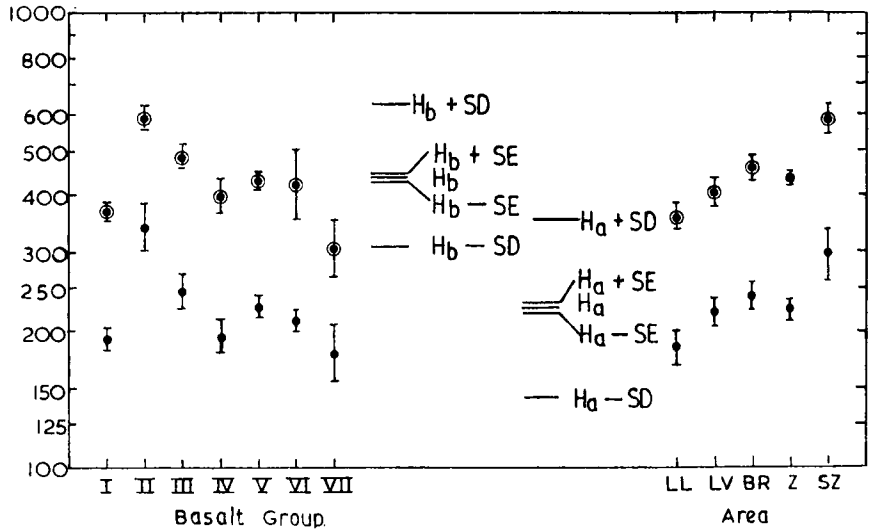

FIG. 17. A.F. coervicities (estimates H_a and H_b as defined in Section 2 of text) computed for each group of flows and also for each area of collection. Overall means with their standard errors and standard deviations also shown.

Mean A.F. coercivities standard errors shown for group and area means: SD = standard deviation and SE = standard error of overall means.

10. Conclusions

10.1. These basalts, whose age ranges from Miocene to Ur. Holocene have been provisionally assigned to geomagnetic polarity epochs as shown in Table 2.

10.2. As a result of this classification, we have suggested that certain modifications to the stratigraphical ages are necessary. These suggestions have since been substantiated by K–Ar radiometric age data (Valencio *et al.* 1969).

10.3. The average directions of the cleaned remanence are axial and dipolar at the 95 per cent level of probability. Nevertheless, there exist some flows which possess a stable remanence with directions significantly different from the axial dipole field.

10.4. The secular variations of the geomagnetic field in this part of Argentina during the Brunhes and Matuyama epochs as deduced from the scatter of palaeogeomagnetic field directions are similar to world average values for the same epochs deduced by the same methods (Table 5).

10.5. Electron microprobe analyses of homogeneous titanomagnetite grains and of areas covering many lamellae in exsolved titanomagnetite grains indicate that the molecular proportion of ulvospinel lies between 50 and 75 per cent (Table 6).

10.6. A relationship between oxidation stage and type of thermomagnetic curve has been noted. Basalts with apparently homogeneous titanomagnetites of oxidation stage 1 have either a single low (100–250 °C) Curie point or two Curie points of which one is low and the other above 500 °C (Types 1 and 2 $J_s(T)$ curves). Basalts at oxidation stage 2 have either two Curie points (type 2 $J_s(T)$ curves or a single high Curie point ($J_s(T)$ curves of types 3 and 4). Basalts at oxidation stage 3, 4 or 5 have only a single high Curie point (type 3 or 4 $J_s(T)$ curves) (see Table 7).

10·7. Analyses of pairs of samples from the same flow with high and low stability to demagnetization by the alternating magnetic field method reveal that the one with

higher stability invariably (a) is of the higher degree of oxidation (Table 8), (b) has the smaller NRM intensity and (c) exhibits the higher Curie temperature.

10.8. Although no special effort was made to investigate whether there exist differences in physical properties between samples from normally and reversely magnetized flows, it can be concluded from the measurements made (a) that no obvious differences in degree oxidation exist (Table 9) and (b) that as far as the NRM intensity of samples with higher coercivity is concerned, those with normal polarity are significantly stronger than those with reversed polarity. This is due to the presence of a stable secondary component in the present normal geomagnetic field direction. Such a difference does not exist between normally and reversely polarized samples with low A.F. coercivity, presumably due to random partial remagnetization between the time of collection and measurement.

10.9. It is tentatively concluded that the intensity of remanence of the basalts varied more with time of extrusion than with geographic area at a given time.

11. Acknowledgments

The authors gratefully acknowledge the encouragement of and financial support for this joint research project by the National Council for Scientific and Technical Investigations of the Republic of Argentina and from the Royal Society of London. We also thank the University of Buenos Aires and Newcastle upon Tyne for laboratory facilities and technical help placed at our disposal in the Departments of Geological Sciences, and of Geophysics and Planetary Physics respectively. Finally we wish to express our thanks to the Exploration Management of Y.P.F. (The Argentine National Oil Company) for having provided a vehicle and driver for carrying out the field work and for allowing us access to unpublished geological information from their files.

K. M. Creer:
School of Physics,
University of Newcastle upon Tyne.

D. A. Valencio:
Department of Geological Sciences,
University of Buenos Aires.

1969 *July.*

References

Creer, K. M., 1958. Preliminary palaeomagnetic measurements in S. America, *Ann. Geophys.*, **14**, 375–389.

Creer, K. M., 1962. The dispersion of the geomagnetic field due to secular variation and its determination in remote times from palaeomagnetic data, *J. geophys. Res.*, **67**, 3461–3476.

Creer, K. M. & Sanver, M., 1968. Secular variations of the geomagnetic field in the Quaternary and late Tertiary, Paper presented at NATO Conference on Palaeogeophysics, University of Newcastle upon Tyne, April 1967, to be published by Academic Press, London and New York.

Creer, K. M. & Ibbetson, J., 1969. Electron probe microanalyses of titanomagnetites in basalts, in preparation.

Creer, K. M. & Petersen, N., 1969. Thermochemical magnetization in Basalts, *Zeit. Geophys.*, in press.

Criado, Roque P., 1949. Relevamiento geologico de la Hoja 29-b, Bardes Plances. Unpublished work, Y.P.F., Buenos Aires.

Frohlich, F., Löffler, H. & Stiller, H., 1965. Interpretation of changes in Curie temperatures observed in rocks, *Geophys. J. R. astr. Soc.*, **9**, 411–422.

Groeber, P., 1929. Lineas fundamentales de la Geologia del Neuquen, Sud de Mendoza y regiones adyacentes. Direcion General de Minas, Publicacion 58.

Groeber, P., 1933. Confluencia de los rios Grande y Barrancas (Mendoza y Neuquen). Descripcion de la Hoja 31a del mapa geologico general de la Republica Argentina. Boletin no 38 de la Direccion de Minas y Geologia.

Groeber, P., 1937. Hoja 30c del Mapa Geologico general de la Republica Argentina. Mapa sin texto; Direccion de Minas y Geologia.

Groeber, P., 1946. Observaciones geologicas a lo largo del meridiano 70: 1. Chos Malal. Revista de la Sociedad Geologica Argentina, Tomo 1, No 3.

Groeber, P., 1947. Observaciones geologicas a lo largo del meridiano 70: 3. Hojas Domuyo, Mari Mahuida, Huarhuar-Co y parte de Epu Lauquen; 4. Hojas Bardas Blancas y Los Molles. Revista de la Sociedad Geologica Argentina, Tomo II, No. 4.

Groeber, P., 1949. Observaciones geologicas a lo large del meridiano 70. Adiciones y correcciones. Revista de la Asociacion Geologica Argentina, Tomo IV, No. 1.

Irving, E. & Ward, M. A., 1964. A statistical model of the geomagnetic field, *Pageoph*, **57**, 47–52.

Lambert, L. R., 1956. Descripcion geologica de la Hoja 35b Zapala (T.N. de Neuquen). Direccion Nacional de Mineria, Boletin No. 83.

Sanver, M., 1968a. Palaeomagnetic study on plio-quaternary rocks, Ph.D. Thesis, University of Newcastle upon Tyne, 249 pp.

Sanver, M., 1968b. A palaeomagnetic study of quaternary rocks from Turkey, *Phys. Earth Planet. Interiors*, **1**, 403–421.

Valencio, D. A., 1965a. Resultados preliminares del estudio palaeomagnetico del Basalto de la Barda Negra. Provincia de Neuquen. Revista de la Asociacion Geologica Argentina, Tomo XX, No. 1.

Valencio, D. A., 1965b. Estudio paleomagnetico del Basalto II de edad suprapliocena de la Pampa de Zapala, Provincia de Neuquen. Revista de la Asociacion Geologica Argentina, Tomo XX, No. 2.

Valencio, D. A. & Creer, K. M., 1968. El Paleomagnetismo de algunas lavas Cenozoicas de la Republica Argentina, Revista Asoc. Geol. Argentina, **23**, 255–278.

Valencio, D. A., Linares, E. & Creer, K. M., 1969. Paleomagnetism and K-Ar ages of Cenozoic basalts from Argentina, *Geophys. J. R. astr. Soc.* **19**, 147–164.

Watson, G. S. & Irving, E., 1957. Statistical methods in rock magnetism, *Mon. Not. R. astr. Soc. Geophys. Suppl.*, **7**, 289–300.

Wilson, R. H. & Watkins, N., 1967. Correlation of petrology and natural remanent polarity in Colombia Plateau basalts, *Geophys. J. R. astr. Soc.*, **12**, 405–424.

Zollner, W. & Amos, A. J., 1953. Descripcion Geologica de la Hoja 32b. Chos Malal. Unpublished. Department of Mines and Geology, Buenos Aires.